Applied Radiation and Isotopes 153 (2019) 108817

Contents lists available at ScienceDirect

Applied Radiation and Isotopes

journal homepage: www.elsevier.com/locate/apradiso

Spectrometry analysis algorithm based on R-L deconvolution and fuzzy inference

Zeyu Wang[a], Pin Gong[a,b], Dajian Liang[a], Xiaobin Tang[a,b,*], Peng Wang[c], Jinzhao Zhang[d], Le Gao[a], Rui Zhang[a]

[a] Department of Nuclear Science & Engineering, Nanjing University of Aeronautics and Astronautics, Nanjing, 210016, China
[b] Jiangsu Key Laboratory of Nuclear Energy Equipment Materials Engineering, Nanjing University of Aeronautics and Astronautics, Nanjing, 210016, China
[c] School of Environmental and Biological Engineering, Nanjing University of Science and Technology, Nanjing, 210094, China
[d] National Ocean Technology Center, Tianjin, 300112, China

HIGHLIGHTS

- A spectrometry analysis algorithm based on Richardson-Lucy (R-L) deconvolution and fuzzy inference is developed.
- The algorithm improves radionuclide identification from low-resolution gamma-ray spectra.
- The method was experimentally tested showing enhanced identification performance.

ARTICLE INFO

Keywords:
R-L deconvolution
Fuzzy inference
Peak-search
Spectrometry analysis
Radionuclide identification

ABSTRACT

A spectrometry analysis algorithm based on Richardson-Lucy (R-L) deconvolution and fuzzy inference is developed to identify radionuclides of overlapping spectra obtained by a low-resolution detector. The effectiveness of the algorithm was experimentally verified. It is shown that the algorithm can be used for radionuclide analysis of low-resolution spectra in a marine environment with high accuracy of nuclide identification.

1. Introduction

Identifying low-level radionuclides released from nuclear facilities is challenged by the presence of a large number of natural radionuclides of relatively high concentration, e.g. ^{40}K (11–12 Bq/L) (Kusakabe, 2017). The Compton continuum associated with these natural nuclides generates high background counts in the low energy tail of the spectrum, suppressing some photopeaks required to identify radionuclides. Marine radioactivity monitoring employs detectors such as HPGe (Povinec et al., 1996), $LaBr_3$ (Su et al., 2011), or NaI(Tl) (Eleftheriou et al., 2013). However, the low detection efficiency of HPGe detectors and the need to cool them limits their use. The radioactivity (1.5 Bq/cc) generated by $LaBr_3$ itself affects its nuclide identification ability (Menge et al., 2007). NaI(Tl) detectors have the advantages of robustness and high detection efficiency, in addition to being relatively cheap. However, the low energy resolution of the NaI(Tl) detectors causes overlap between close photopeaks used to identify radionuclides (Chen and Wei et al., 2009).

Spectrum deconvolution with a predetermined detector response is an effective means to resolve overlapping indications for improving resolution (see for example, Beach et al., 2007). In particular, Richardson-Lucy (R-L) deconvolution has been proved to be effective in suppressing Poisson noise, and it is easier to extract peak features from a deconvoluted spectrum (Morháč and Matoušek, 2011). The purpose of deconvolution is to obtain the peak energy distribution under ideal conditions, but the deconvolution of the spectrum with the detector-response matrix may result in additional erroneous peaks (Beach et al., 2007). We propose here the use of fuzzy inference system to eliminate theses false peaks.

Fuzzy inference has the ability to produce a credible output from incomplete, fuzzy or inaccurate input by simulating human decision-making (Zadeh, 1988). Alamaniotis et al. (2013) were the first to use fuzzy inference in gamma-ray spectroscopy. In this paper, we propose to combine R-L deconvolution with fuzzy inference system. To demonstrate the concept, the algorithm was applied to the environmental background spectrum and test spectrum of ^{241}Am in laboratory

* Corresponding author. Nanjing University of Aeronautics and Astronautics, Nanjing, 210016, China.
E-mail address: tangxiaobin@nuaa.edu.cn (X. Tang).

https://doi.org/10.1016/j.apradiso.2019.108817
Received 6 December 2018; Received in revised form 19 July 2019; Accepted 19 July 2019
Available online 23 July 2019
0969-8043/

environment. Then, the feasibility of this algorithm in low activity environment was verified against an ocean background spectrum.

2. Methodology

Before performing spectrum analysis, a detector was used to measure the gamma-ray spectra and the natural background spectra. Wavelet transform was then used for noise reduction to eliminate the influence of ambient interference noise by approximate coefficient extraction and normalization (He et al., 2018). R-L deconvolution was subsequently used to process the denoised gamma-ray spectrum. A photopeak-search algorithm was then applied to determine peak positions (energies). The list of the photopeaks were processed, together with a nuclide library of radionuclides, using fuzzy inference, to determine the degree of matching between the characteristic peaks of nuclides in the nuclide library and the searched peaks. The matching degree was subsequently adjusted by setting constraints of energy and counts to finalize the list of detected nuclide lists and the corresponding identification confidences. Further details are given below.

A spectrum can be expressed as:

$$\boldsymbol{y} = \boldsymbol{H}^{*}\boldsymbol{x} + \boldsymbol{b} \quad (1)$$

where $\boldsymbol{y}$ is an $N \times 1$ vector representing the measured spectrum, $\boldsymbol{x}$ is the ideal radionuclide spectrum, $\boldsymbol{b}$ defines the background spectrum, and the matrix $\boldsymbol{H}$ is the detector response matrix of dimensions NN. R-L deconvolution (Morháč and Matoušek, 2011) is expressed as:

$$p(x|y) = \frac{p(y|x)p(x)}{p(y)} \quad (2)$$

$$x^{(n+1)}(i) = x^{(n)}(i) \sum_{j=0}^{N-1} h(j,i) \frac{y(i)}{\sum_{k=0}^{M-1} h(j,k)x^{(n)}(k)} \quad (3)$$

where $p(x)$ denotes the probability that of radionuclides being detected, $p(y)$ is the probability of these nuclides being recorded in the measured spectrum, and $h(j,i)$ is an the element of $\boldsymbol{H}$ with $i,j = 1, \ldots N$.

By iteration via Eq. (3), the R-L algorithm converges to the maximum likelihood of $\boldsymbol{x}$. The response matrix, $\boldsymbol{H}$, for a 76.2 mm × 76.2 mm NaI detector (ORTEC Inc.) was obtained using convolution of the energy deposition spectra with the detector resolution function (Klusoň and Jánský, 2010). The number of iterations was set to be 10,000 as was done by Morháč and Matoušek (2011).

The peak-search algorithm first finds all potential peaks, P_i, then marks the peak positions, peak counts and net counts. The Statistics-sensitive Non-linear Iterative Peak-clipping (SNIP) algorithm was used to deduct the background spectra to obtain the net peak counts. The ratio, P_{ir}, between net counts and peak counts of all potential peaks is calculated. A threshold, T_p, is applied to all peak positions to remove some erroneous peaks, and it is not a fixed value. The default value of T_p in this study was set to 0.1, i.e., the accepted net count (after subtracting the background) at a peak position has to be greater than or equal to one tenth of its gross peak counts. The impact of the threshold setting on the analysis results was analyzed in subsequent experiments.

A fuzzy inference system was employing for estimating the level of confidence in determining the presence or absence of radionuclides in an energy spectrum. The input of this system was the absolute value of the energy difference between the characteristic peak, E_{ij}, in the nuclide library and the potential peak, P_i, closest to E_{ij}, and the output is the confidence level, C_{ij}, of the characteristic peak. Fuzzy rules were formulated as the following if-then rule statements:

If (Energy Difference is Small), then (Identification Confidence is High)

If (Energy Difference is Middle), then (Identification Confidence is Modest)

If (Energy Difference is Large), then (Identification Confidence is Low).

A process of defuzzification is then applied to map the fuzzy set output to an accurate output. If one peak position, P_i, matches multiple characteristic peak positions in the nuclide library, constraint conditions were set by first finding the peak lists, $P_{i,template}$, in the background spectrum, then setting a threshold of energy difference, T_{gap}, and net count ratio, T_{ratio}, finding the nearest peak from $P_{i,template}$ for P_i, and calculating the ratio, R, between net counts of P_i and $P_{i,template}$, so that:

$$if\ |P_i - P_{i,template}| \le T_{gap}\ and\ R > T_{ratio}$$

This reserves the detection certainty of the characteristic peak of a natural radionuclide in the nuclide library which matches the peak, P_i, and resets the detection certainty of the characteristic peak of other radionuclides in nuclide library which matches P_i to 0. The conditions:

$$if\ |P_i - P_{i,template}| \le T_{gap}\ and\ R \le T_{ratio}$$

$$or$$

$$if\ |P_i - P_{i,template}| > T_{gap}$$

reserve the detection certainty of the characteristic peak of a natural radionuclide in the nuclide library which matches the peak, P_i, and the characteristic peak of an unnatural radionuclide which matches the peak, P_i, with highest detection certainty, and resets the detection certainty of the characteristic peak of other radionuclides in nuclide library which matches P_i to 0. Based on gamma-ray spectrum analysis experiments of ^{60}Co and ^{137}Cs under different measurement conditions, T_{gap} and T_{ratio} were, respectively, set to 20 keV and 1.1 in this study.

The identification confidences, C_{ij}, for all characteristic peaks in the nuclide library were constrained, and the peak position identification confidences were converted into nuclide identification confidences by

$$C_i = \frac{\sum_{j=1}^{m} W_{ij} \times C_{ij}}{\sum_{j=1}^{m} W_{ij}} \quad (4)$$

where W_{ij} indicates the weight of the j-th characteristic peak of the i-th nuclide, m indicates the number of characteristic peaks of the i-th nuclide (Alamaniotis and Tsoukalas, 2015). The weight is the proportion of each characteristic peak in the nuclide, which is a known value (Ansi et al., 2007). The value of the confidence ranges from 0 to 1, and the higher the confidence, the greater the possibility of the presence of this nuclide in the spectrum. Therefore, the confidence threshold was set to 0.9 based on the experimental analysis of ^{60}Co and ^{137}Cs spectra. The value of an identification confidence greater than 0.9 indicates that it is recognized by the system.

3. Results and analysis

A spectroscopy system consisting of a 76 mm × 76 mm NaI(Tl) detector (ORTEC Inc.) with a resolution of approximately 7.7% at 662 keV, was used. A program based on the SDK in the MAESTRO software (ORTEC Inc.) was written to obtain the gamma-ray spectra. The radioactive source used in algorithm performance testing was ^{241}Am (9.435×10^{-3} MBq).

The natural background spectrum in these experiments was recorded over 3600 s in the laboratory using a NaI(Tl) detector. Two methods were applied, for comparison. In the first method, the energy spectrum was preprocessed by wavelet transform, the peak-search algorithm was directly used to extract peak positions information, then nuclide identification was carried out by fuzzy inference without deconvolution. In the second method, the energy spectrum was first preprocessed by wavelet transform, followed by deconvolution, then peak positions information was extracted by peak-search algorithm, subsequently nuclide identification was performed by fuzzy inference matching the peak positions information of the nuclide library. The nuclide library consisted of the following natural background nuclides: ^{40}K, ^{226}Ra, ^{214}Bi, ^{214}Pb, ^{228}Ac, ^{212}Pb, and ^{208}Tl.

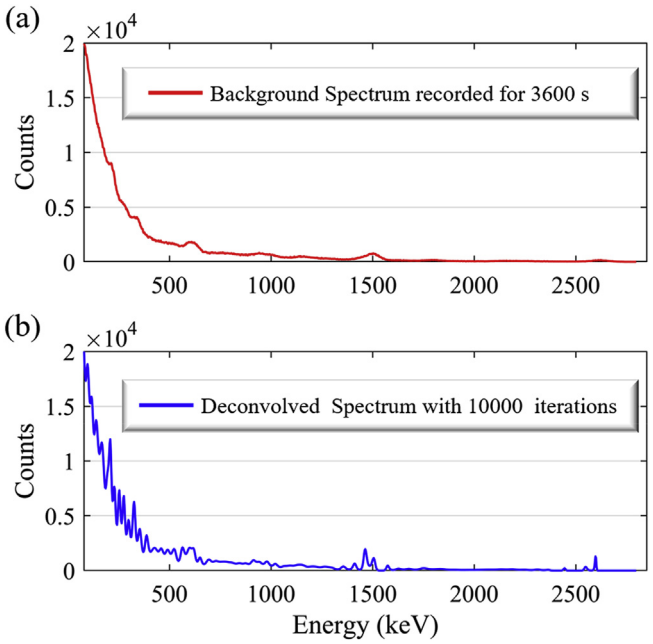

Fig. 1. Effect of the R-L deconvolution algorithm applied to the natural background spectrum. **(a)** Natural background spectrum and **(b)** Background spectrum processed by the R-L algorithm.

The measured background spectrum contained a relatively high count in the low-energy region due to the noise of photomultiplier tube and Compton scattering, and a small portion of the background spectrum in the low energy region (about < 30 keV) was removed in the spectrum analysis. Through deconvolution with the detector-response matrix ***H***, many small peaks (even though some of them were erroneous peaks) appeared in the background spectrum in Fig. 1.

Table 1 shows the identification results from the natural background spectrum, including the matching peak positions of all characteristic peaks, the identification confidences of peak positions, and the identification confidences of nuclides. Fuzzy inference nuclide identification applied to the natural background spectrum without deconvolution was carried out, only two radionuclides (^{40}K and ^{212}Pb) were identified with the confidence higher than the threshold (0.9), as shown in Part A of Table 1. In the process of nuclide identification, a situation occurred in which a peak position matched multiple characteristic peaks. According to the constraint conditions, the mismatched characteristic peaks were eliminated by energy difference and net count rate, and their identification confidences were reset to 0 to reduce the error recognition rate. It should be noted that the identification confidences of the seven nuclides (^{40}K, ^{226}Ra, ^{214}Bi, ^{214}Pb, ^{228}Ac, ^{212}Pb, and ^{208}Tl) were higher than threshold (0.9), when the energy spectrum was subjected to deconvolution processing and then identified by fuzzy inference, as shown in Part B of Table 1. The results show that the introduced algorithm can identify radionuclides present in the low-resolution natural background spectrum with high confidence. That is to say, the R-L deconvolution algorithm in effect enhances the energy resolution and improves the performance of nuclide identification together with fuzzy inference.

The algorithmic performance was also tested in an experiment in which by an ^{241}Am (9.435×10^{-3} MBq) source was placed in front of the detector and its spectrum was recorded over a period of 300 s. The distance from the detector to the source ranged from 100 to 500 mm with an interval of 100 mm. The test spectra were first processed by wavelet transform, followed by deconvolution, and then the background was subtracted by SNIP algorithm. Nuclide identification was then performed by fuzzy reasoning. The raw spectrum curve with a detection distance of 100 mm, shown in Fig. 2, clearly showed the

Table 1
Identification results from a natural background spectrum.

Part A: Identification from the raw natural background spectrum without deconvolution

Nuclide	Characteristic Peak (keV)	Matching Peak (keV)	Confidence of Peak	Confidence of Nuclide
^{214}Bi	609.3	665.2853	0.505	0.730
	1764	1761.5397	0.990	
	1120.3	1117.5260	0.990	
	1238	1237.7419	1	
	768.4	745.4293	0.885	
^{208}Tl	2614.5	2614.5	1	0.768
	583.1	539.3449	0.500	
^{226}Ra	186.1	132.9007	0.505	0.505
^{228}Ac	911.1	905.7171	0.975	0.747
	969.1	948.6514	0.900	
	338	419.129	0	
^{40}K	1460.8	1466.725	0.970	0.970
^{214}Pb	351.9	419.129	0	0.330
	295.2	250.2543	0.500	
^{212}Pb	238.6	250.2543	0.945	0.945

Part B: Identification from the natural background spectrum after deconvolution

Nuclide	Characteristic Peak (keV)	Matching Peak (keV)	Confidence of Peak	Confidence of Nuclide
^{214}Bi	609.3	634.2303	0.920	0.911
	1764	1753.637	0.965	
	1120.3	1134.27	0.955	
	1238	1259.28	0.930	
	768.4	679.6884	0.505	
^{208}Tl	2614.5	2614.5	1	1
	583.1	583.09	1	
^{226}Ra	186.1	185.33	1	1
^{228}Ac	911.1	901.3	0.970	0.982
	969.1	969.48	1	
	338	333.07	0.985	
^{40}K	1460.8	1461	1	1
^{214}Pb	351.9	367.16	0.950	0.957
	295.2	304.66	0.970	
^{212}Pb	238.6	230.79	0.975	0.975

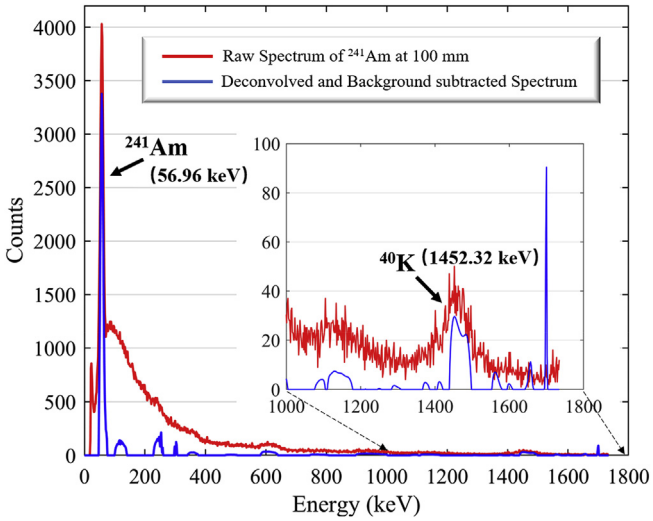

Fig. 2. Raw spectrum of ^{241}Am at 100 mm and the spectrum processed by deconvolution and the SNIP algorithm.

characteristic photopeak of ^{241}Am, and the identification confidence of ^{241}Am was 0.995, higher than threshold (0.9). The same results were observed in experiments with detection distances of 200, 300, and 400 mm. The increase in distance is equivalent to observing a weaker source activity.

The raw spectrum of ^{241}Am at 500 mm was similar to the natural

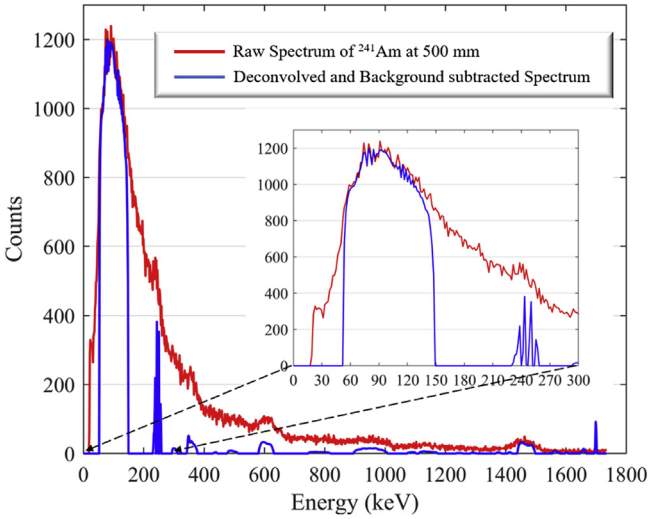

Fig. 3. Raw spectrum of ^{241}Am at 500 mm and the spectrum processed by deconvolution and the SNIP algorithm.

Table 2
Identification results from the ^{241}Am spectrum.

Part A: Identification from the raw spectrum without deconvolution

Nuclide	Characteristic Peak (keV)	Matching Peak (keV)	Confidence of Peak	Confidence of Nuclide
^{241}Am	59.54	92.87	0	0
^{214}Bi	609.3	602.45	0.980	0.794
	1764	1587.41	0	
	1120.3	1137.68	0.945	
	1238	1262.51	0.920	
	768.4	773.45	0.985	
^{208}Tl	2614.5	1587.41	0	0.268
	583.1	602.45	0.500	
^{226}Ra	186.1	241.64	0	0
^{228}Ac	911.1	956.42	0	0.284
	969.1	956.42	0.960	
	338	352.79	0	
^{40}K	1460.8	1469.42	0.975	0.975
^{214}Pb	351.9	352.79	1	0.993
	295.2	301.49	0.98	
^{212}Pb	238.6	241.64	0.99	0.990

Part B: Identification from the spectrum with deconvolution and fuzzy reasoning

Nuclide	Characteristic Peak (keV)	Matching Peak (keV)	Confidence of Peak	Confidence of Nuclide
^{241}Am	59.54	62.09	0.995	0.995
^{214}Bi	609.3	597.32	0.960	0.882
	1764	1698.56	0.500	
	1120.3	1129.13	0.970	
	1238	1247.12	0.970	
	768.4	770.03	0.995	
^{208}Tl	2614.5	1698.56	0	0
	583.1	597.32	0	
^{226}Ra	186.1	238.22	0	0
^{228}Ac	911.1	930.77	0.935	0.756
	969.1	966.68	0.995	
	338	347.66	0	
^{40}K	1460.8	1452.32	0.975	0.975
^{214}Pb	351.9	347.66	0.985	0.982
	295.2	303.20	0.975	
^{212}Pb	238.6	238.22	1	1

background spectrum, and the photopeak of ^{241}am was not as visible due to the low counts, as shown in Fig. 3. The raw spectrum was firstly smoothed by wavelet transform, then the background was subtracted by the SNIP algorithm, and then nuclide identification was conducted by peak-search algorithm and fuzzy inference without deconvolution. Part A in Table 2 shows the identification results using fuzzy inference applied to the background-subtracted spectrum without deconvolution. A total of 14 peak positions were matched. The identification confidence for ^{40}K, ^{212}Pb, and ^{214}Pb was higher than the threshold (0.9), indicating that they were identified. However, all other radionuclides, including ^{241}Am, were not identified. The low energy and low-radioactivity of ^{241}Am caused it to be concealed by the natural background radiation. Subsequently, we performed a complete algorithm analysis for the raw spectrum with deconvolution and fuzzy reasoning. A total of 29 peak positions were matched, and the matching peak of ^{241}Am was 62.09 keV with a confidence of 0.995. The net count rate of ^{241}Am was $6.53 \pm 1.86 s^{-1}$.

As the count rate of ^{241}Am decreased further, its characteristic peak becomes too small to be recognized, even after deconvolution. Therefore, the minimum number of counts that have to be registered that allows the methodology to analyze the spectrum should be greater than about $7 s^{-1}$. The complete identification results were provided in Part B of Table 2. When the threshold, T_p, in the peak-search algorithm was increased from 0.1 to 0.18, the matching peak of ^{241}Am changed to 74.06 keV, and the confidence level was lower than the threshold (0.9). As the threshold becomes larger, the ratio, P_{ir}, for some potential peaks is smaller than T_p, resulting in the peak being eliminated and not fed into the fuzzy inference system. Therefore, the threshold, T_p, has a great influence on the results of nuclide identification, which needs to be analyzed and set according to experimental conditions.

Finally, the feasibility of the algorithm in marine environment was verified. The test spectrum was obtained with the help of the National Ocean Technology Center (NOTC, Tianjin, China) by placing the detector 400 m below sea level and recording the spectrum for 34 h. The raw spectrum was deconvoluted and then identified by fuzzy inference. Table 3 shows the identification results of the deconvoluted spectrum of Fig. 4 using fuzzy inference. A total of 38 peak positions were matched. The nuclides that contribute the most to the natural background in the marine environment are ^{40}K, ^{214}Bi, ^{214}Pb, and the confidence level for ^{40}K and ^{214}Bi was higher than the threshold (0.9). The matching peak for ^{137}Cs was 631.5 keV, and the confidence was lower than the threshold (0.9), indicating that the sea area was not affected by the nuclear power plant effluent. This experiment confirmed that deconvolution algorithm and fuzzy inference system can be applied to the low activity spectrum analysis and accurately identify the radioisotopes in the marine environment.

4. Conclusions

A low-resolution spectrometry analysis algorithm based on R-L deconvolution and fuzzy inference was proposed in this study. The

Table 3
Identification results from ocean background spectrum.

Nuclide	Characteristic Peak (keV)	Matching Peak (keV)	Confidence of Peak	Confidence of Nuclide
^{137}Cs	661.7	631.473	0	0
^{40}K	1460.8	1450.608	0.965	0.965
^{214}Pb	351.9	358.428	0.980	0.817
	295.2	250.713	0.500	
^{212}Pb	238.6	238.188	1	1
^{214}Bi	609.3	603.918	0.985	0.942
	1764	1758.723	0.985	
	1120.3	1144.998	0.920	
	1238	1300.308	0.500	
	768.4	771.753	0.990	
^{208}Tl	2614.5	2530.263	0.505	0.723
	583.1	591.393	0.975	
^{226}Ra	186.1	220.653	0.885	0.885
^{228}Ac	911.1	942.093	0.900	0.728
	969.1	957.123	0.960	
	338	358.428	0	

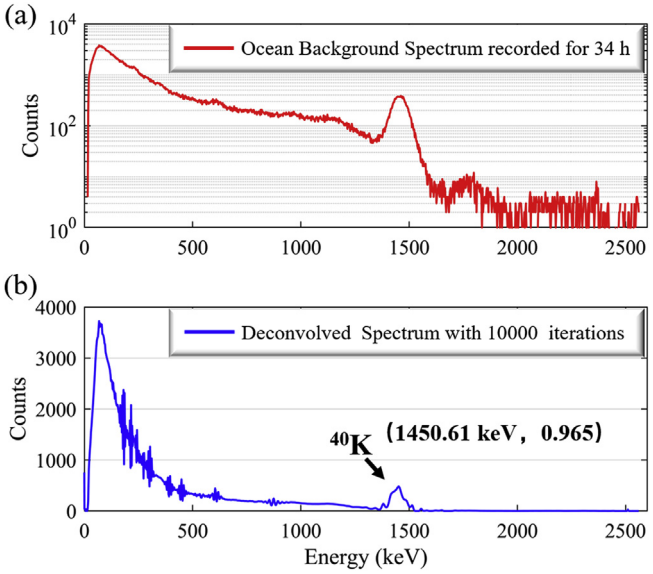

Fig. 4. (a) Raw natural background in the marine environment (b) deconvolution spectrum with 10000 iterations.

algorithm was test experimentally, showing that it can accurately identify radionuclides in a low-resolution spectrum when it meets the minimum detectable value of radionuclides (about $7s^{-1}$ for ^{241}Am). The application of the deconvolution algorithm in effect enhances the energy resolution and helps to increase the number of identified radionuclides from 2 to 7 in a natural background spectrum. In addition, optimizing the threshold of the peak search algorithm and fuzzy reasoning improved the accuracy of nuclide identification. The energy spectrum analysis algorithm was successfully applied to a natural low-resolution spectrum both in the laboratory and in a marine environment.

Acknowledgments

This work was supported by the National Natural Science Foundation of China (Grant No. 11675078), the Primary Research and Development Plan of Jiangsu Province, China (Grant No. BE2017729), the Funding of Jiangsu Innovation Program for Graduate Education, China (Grant No. KYLX16_0353, No. kfjj20180601).

References

Alamaniotis, M., Jevremovic, T., 2015. Hybrid fuzzy-genetic approach integrating peak identification and spectrum fitting for complex Γ-ray spectra analysis. IEEE Trans. Nucl. Sci. 62, 1262–1277. https://doi.org/10.1109/TNS.2015.2432098.

Alamaniotis, M., Heifetz, A., Raptis, A.C., Tsoukalas, L.H., 2013. Fuzzy-logic radioisotope identifier for gamma spectroscopy in source search. IEEE Trans. Nucl. Sci. 60, 3014–3024. https://doi.org/10.1109/TNS.2013.2265307.

Ansi, N., 2007. American National Standard for Evaluation and Performance of Radiation Detection Portal Monitors for Use in Homeland Security. pp. c1–35.

Beach, S.M., DeWerd, L.A., 2007. Deconvolution and reconstruction techniques of closely spaced low-energy spectra from high-purity germanium spectrometry. Nucl. Instrum. Methods Phys. Res. A. 572, 794–803. https://doi.org/10.1016/j.nima.2006.12.006.

Chen, L., Wei, Y.X., 2009. Nuclide identification algorithm based on K–L transform and neural networks. Nucl. Instrum. Methods Phys. Res. A. 598, 450–453. https://doi.org/10.1016/j.nima.2008.09.035.

Eleftheriou, G., Tsabaris, C., Androulakaki, E.G., Patiris, D.L., Kokkoris, M., Kalfas, C.A., Vlastou, R., 2013. Radioactivity measurements in the aquatic environment using in-situ and laboratory gamma-ray spectrometry. Appl. Radiat. Isot. 82, 268–278. https://doi.org/10.1016/j.apradiso.2013.08.007.

He, J.P., Tang, X.B., Gong, P., Wang, P., Han, Z.Y., Yan, W., Gao, L., 2018. Spectrometry analysis based on approximation coefficients and deep belief networks. Nucl. Sci. Tech. 29, 69. https://doi.org/10.1007/s41365-018-0402-4.

Klusoň, J., Jánský, B., 2010. Calculation of responses and analysis of experimental data for a silicon gamma spectrometer. Nucl. Instrum. Methods Phys. Res. A. 619, 186–189. https://doi.org/10.1016/j.nima.2009.10.180.

Kusakabe, M., 2017. Distributions of radionuclides in the ocean and their temporal changes. Rep. Mar. Ecol. Res. Inst. 22, 3–16.

Menge, P.R., Gautier, G., Iltis, A., Rozsa, C., Solovyev, V., 2007. Performance of large lanthanum bromide scintillators. Nucl. Instrum. Methods Phys. Res. A. 579 (1), 6–10. https://doi.org/10.1016/j.nima.2007.04.002.

Morháč, M., Matoušek, V., 2011. High-resolution boosted deconvolution of spectroscopic data. J. Comput. Appl. Math. 235, 1629–1640. https://doi.org/10.1016/j.cam.2010.09.005.

Povinec, P.P., Osvath, I., Baxter, M.S., 1996. Underwater gamma-spectrometry with HPGe and NaI(Tl) detectors. Appl. Radiat. Isot. 47, 1127–1133. https://doi.org/10.1016/S0969-8043(96)00118-2.

Su, G., Zeng, Z., Cheng, J., 2011. Monte Carlo simulation of in situ LaBr gamma-ray spectrometer for marine environmental monitoring. Radiat. Prot. Dosim. 146, 103–106. https://doi.org/10.1093/rpd/ncr122.

Zadeh, L., 1988. Fuzzy logic. Comput. Times 21, 83–93. https://doi.org/10.1109/2.53.